The Journal of Immunology

Homeostatic Lymphoid Chemokines Synergize with Adhesion Ligands to Trigger T and B Lymphocyte Chemokinesis

Agnieszka N. Stachowiak, Yana Wang, Yen-Chen Huang and Darrell J. Irvine

J Immunol 2006; 177:2340-2348; ;
doi: 10.4049/jimmunol.177.4.2340
http://www.jimmunol.org/content/177/4/2340

The Journal of Immunology is published twice each month by
The American Association of Immunologists, Inc.,
1451 Rockville Pike, Suite 650, Rockville, MD 20852

Print ISSN: 0022-1767 Online ISSN: 1550-6606.

Homeostatic Lymphoid Chemokines Synergize with Adhesion Ligands to Trigger T and B Lymphocyte Chemokinesis[1]

Agnieszka N. Stachowiak,* Yana Wang,† Yen-Chen Huang,*‡ and Darrell J. Irvine[2]*‡

Homeostatic chemokines such as CCL19, CCL21, and CXCL13 are known to elicit chemotaxis from naive T and B cells and play a critical role in lymphocyte homing to appropriate zones within secondary lymphoid organs (SLO). Here we tested whether CCL21 and CXCL13 modulate murine lymphocyte motility in the absence of concentration gradients, using videomicroscopy to directly observe the migration of single cells. CCL21 treatment of T cells induced rapid polarization and sustained random migration with average speeds of 5.16 ± 2.08 μm/min; B cell migration (average velocity 4.10 ± 1.58 μm/min) was similarly induced by CXCL13. Migration required the presence of both chemokine and adhesion ligands and was sustained for >24 h. Furthermore, in in vitro assays modeling the relative infrequency of Ag-specific T cell-dendritic cell (DC) encounters during primary immune responses, we found that CCL21 addition to T-DC cocultures accelerated the kinetics of CD69 up-regulation and enhanced by 2-fold the proliferation of Ag-specific T cells in a manner dependent on G-protein-coupled receptor signaling in T cells. These results suggest that homeostatic chemokines could substantially impact the dynamics and priming of lymphocytes within SLO even in the absence of significant concentration gradients. *The Journal of Immunology,* **2006, 177: 2340–2348.**

Time-lapse fluorescence imaging of intact murine lymph nodes has revealed that T and B cells exhibit dramatic, sustained motility during homeostasis and during some phases of Ag priming, which may be critical for efficient Ag surveillance (Refs. 1–3 and reviewed in Refs. 4 and 5). The polarized, migrating phenotype of naive lymphocytes in vivo is likely supported by signals present in the tissues, because T and B cells isolated from murine secondary lymphoid organs (SLO)[3] or human PBL are largely rounded and non-motile, even if cultured in contact with some adhesive substrates (4, 6–8). Homeostatic chemokines produced constitutively in SLO, such as CCL21, CCL19, CXCL13, and CXCL12, probably play a key role in regulating lymphocyte motility in these tissues. Lymphocytes migrate up concentration gradients of these chemokines in vitro, and such chemotaxis may be involved in their directed transit across high endothelial cells (from blood to lymph nodes), where pronounced chemokine concentration gradients might be encountered.

However, chemotaxis need not be the only mechanism for chemokines to regulate lymphocyte motility in SLO; at uniform concentrations, chemoattractants may also increase the velocity of cell migration. The rapid, apparently randomly directed migration of T and B cells observed in vivo (1, 2, 4) could be the result of short-range direction and redirection in response to very localized chemokine gradients within the T cell and B cell areas (9), or alternatively, could represent a chemokinetic response to near-uniform levels of chemokine in the tissue. In vitro, Kaiser et al. recently reported that CCL19 secreted by mature dendritic cells (DC) stimulated pronounced motility in cocultured human naive T cells; addition of soluble CCL19 at uniform concentrations to naive T cells cultured on immature DC (which do not produce CCL19) elicited a similar induction of random motility (8). In light of the evidence, we hypothesized that chemokinesis triggered by homeostatic chemokines could be a general mechanism supporting steady-state lymphocyte motility within SLO.

Notably, in the first studies examining the effects of homeostatic chemokines on lymphocyte migration, chemokinesis was not observed (10–12). However, these in vitro studies used modified Boyden chamber assays, in which cells migrate across a thin porous membrane in response to chemoattractant; the type of migration elicited is assessed by introducing chemokine either to the culture chamber opposite the cells (to assay chemotaxis) or at equal concentrations on both sides of the membrane (for chemokinesis). The use of such "checkerboard" filterplate assays to detect and distinguish between types of migration can be problematic (13), and in some cases, factors that appeared to be only chemotactic in such assays have shown clear chemokinetic effects when more direct assays of cell migration were employed (14).

We thus used direct videomicroscopic observation to test whether the two most abundant chemokines in the T cell and B cell areas of lymph nodes and spleen, CCL21 and CXCL13, respectively, trigger chemokinesis in resting murine lymphocytes. We found that this was the case, and furthermore, in in vitro assays designed to model the relative infrequency of Ag-specific T cell-Ag-bearing DC encounters that occur during primary immune responses, we found that treatment of T-DC cocultures with CCL21 led to an early enhancement in CD69 up-regulation kinetics and a 2-fold enhancement in the number of Ag-specific T cells recovered after 4 days. These results provide a possible explanation for the lack of naive murine lymphocyte motility in purified cultures relative to their behavior in lymphoid organs and suggest that the high levels of chemokines present in SLO do not require concentration gradients to have a significant impact on lymphocyte migration.

*Department of Materials Science and Engineering, †Department of Chemical Engineering, and the ‡Biological Engineering Division, Massachusetts Institute of Technology, Cambridge, MA 02139

Received for publication November 22, 2005. Accepted for publication May 25, 2006.

The costs of publication of this article were defrayed in part by the payment of page charges. This article must therefore be hereby marked *advertisement* in accordance with 18 U.S.C. Section 1734 solely to indicate this fact.

[1] This work was supported by the Whitaker Foundation (Grant no. RG-02-0837) and Defense Advanced Research Planning Agency (award W81XWH-04-C-0139).

[2] Address correspondence and reprint requests to Dr. Darrell J. Irvine, Massachusetts Institute of Technology, Room 8-425, 77 Massachusetts Avenue, Cambridge, MA 02139. E-mail address: djirvine@mit.edu

[3] Abbreviations used in this paper: SLO, secondary lymphoid organs; DC, dendritic cell; FN, fibronectin; iDC, immature DC; OVA-mDC peptide-bearing mature DC; PTX, pertussis toxin.

0022-1767/06/$02.00

Materials and Methods

Cell isolation

All animal work was approved by the MIT Committee on Animal Care, in accordance with federal, state, and local regulations. C57BL/6, OT-II, and GFP BL/6 transgenic mice were obtained from The Jackson Laboratory. DC were derived from the bone marrow of C57BL/6 mice after the procedure of Inaba et al. (15), cultured with 5 ng/ml GM-CSF (R&D Systems), and used on day 7. $CD4^+$ T cells were isolated from spleens or lymph nodes of 6- to 12-wk-old mice by MACS negative selection ($CD4^+$ T cell isolation kit; Miltenyi Biotec), yielding >90% $CD4^+$ cells, >60% $CD62L^{high}CD44^{low}$ naive T cells. For some experiments, cells were further purified: $CD4^+$ T cells were separated into $CD62L^+$ and $CD62L^-$ fractions by MACS positive selection ($CD4^+CD62L^+$ T cell isolation kit; Miltenyi Biotec) or were sorted into $CD62L^+CD44^{low}$ and $CD62L^+CD44^{high}$ populations on a FACSAria (BD Biosciences). B cells isolated by MACS negative selection (B cell isolation kit; Miltenyi Biotec) were typically >85% $B220^+MHCII^+$. Cells were cultured in RPMI 1640 medium supplemented with 10% FCS, 10 mM HEPES, 100 U/ml penicillin, 100 μg/ml streptomycin, 2 mM L-glutamine, and 50 μM 2-ME.

Cell treatments

Cells were incubated with 1–10,000 ng/ml recombinant mouse CCL19 or CCL21 (R&D Systems) for 20 min before initiation of imaging to allow the chemokine to take full effect. PMA treatment (Sigma-Aldrich) was performed at 50 ng/ml, with imaging likewise initiated at 20 min. For LFA-1 blocking studies, anti-LFA-1 clone M17/4 or isotype control Ab was used; anti-I-A^b clone AF6–120 was also used for B cells. For Fc block treatment, B cells were incubated with CD16/32 for 10 min on ice before the addition of other reagents. All Abs were obtained from BD Pharmingen and used at 10 μg/ml. In videomicroscopy studies utilizing pertussis toxin (PTX), cells were treated with 100 ng/ml PTX or PTX B oligomer (Sigma-Aldrich) for 10 min at 37°C, washed twice with warm medium, and rested for 90–120 min before use. In coculture studies, both a high dose (100 ng/ml) and a low dose (2 ng/ml) of PTX were tested; results followed the same trends for both doses. For chemokine removal experiments, cells were washed in 10 ml of warm medium, incubated for 1 h in 2 ml of fresh medium under light shaking (<200 rpm), and washed twice more before imaging.

Videomicroscopy tracking of T cell polarization and chemokinesis

Eight-well chambered coverslips (Lab-Tek; Nalge Nunc) were incubated with 5 $\mu g/cm^2$ fibronectin (FN) for 2 h at 21°C, or 10 μg/ml recombinant ICAM-1/Fc or VCAM-1/Fc fusion proteins (R&D Systems) overnight at 4°C, before addition of cells ($2–3 \times 10^6$) and chemokine. A fraction of $CD4^+$ T cells from C57BL/6 mouse spleens (~20%, for ease of automated tracking) were labeled with 2.5 μM fura 2-AM (Molecular Probes) for 25 min at 37°C. Similarly, splenic $CD4^+$ T cells from GFP mice used for chemokine response longevity studies were diluted to 20% with C57BL/6 $CD4^+$ T cells. Fura (for C57BL/6 mice, exc 380 nm, em 510 nm) or green (for GFP mice, excitation 488 nm, emission 510 nm) fluorescence and bright-field images were acquired at 30 s intervals for 40 min on a Zeiss Axiovert 200 epifluorescence microscope equipped with environmental stage (37°C, 5% CO_2) with the aid of Metamorph software (Universal Imaging).

Image analysis

Cell polarization and migration were analyzed with the aid of Metamorph and Volocity (Improvision) software packages. Data were sharpened with the no-neighbors two-dimensional deconvolution algorithm in Metamorph to facilitate cell tracking using Volocity. For each field, 26–44 cells were analyzed (depending on fluorescent cell density) based on intensity thresholding and size exclusion (to rid a small fraction of large cell contaminants); the dead cell population that developed during longevity experiments was excluded from analysis. A cell was scored as polarized at a single time point if its shape factor (4π area/perimeter^2) did not exceed 0.85. To score average population behaviors, polarized cells were defined as those with a shape factor ≤0.85 in ≥15% of observed time points. Migrating cells were defined as polarizing cells with time-averaged velocities ≥4 (T cell) or 3.5 (B cell) μm/min.

T-DC cocultures

All experiments were performed in 96-well round-bottom plates (BD Falcon). To assay CD69 up-regulation, duplicate samples of 2×10^5 total cells were prepared at an overall T/DC ratio of 1:1. A portion of day 6 DC were matured with 1 μg/ml LPS (Sigma-Aldrich) and pulsed with OVA peptide (ISQAVHAA-HAEINEAGR, 500 nM; AnaSpec Corporate) for 16 h, whereas others were left untouched; mixtures of peptide-loaded (and washed) mature DC (OVA-mDC) and immature DC (iDC) were then prepared at a 1:20 ratio. OT-II $CD4^+$ T cells were also diluted 1:9 with C57BL/6 $CD4^+$ T cells. T cells (with or without PTX pretreatment) and DC mixtures were aliquotted in FN-treated wells, briefly centrifuged (1200 rpm, 1–2 min), then placed in culture in the presence or absence of 1 μg/ml CCL21, which was replenished at 48 h. CD69 up-regulation was analyzed at times ranging from 24 to 96 h: duplicate samples were pooled, cells were stained with anti-CD69-FITC, anti-Vα2-PE, and anti-CD4-biotin followed by streptavidin-allophycocyanin, and finally propidium iodide.

The effect of CCL21 on T cell proliferation was assessed by a CFSE dilution assay, using a similar coculture system: OT-II T cells were labeled with 10 μM CFSE for 10 min and washed 3× before mixing with C57BL/6 $CD4^+$ T cells at a 1:9 ratio. Triplicate cocultures of 5×10^5 total cells were prepared at an overall T/DC ratio of 9:1 and an iDC/OVA-mDC ratio of 1:1; 1 μg/ml CCL21 was added at time zero to CCL21-treated cultures. Proliferation in each well was assayed on day 4 by flow cytometry analysis of cultures stained with anti-Vα2-PE, anti-Vβ5-biotin (then streptavidin-allophycocyanin), and propidium iodide. All data was collected on a FACSCalibur (BD Biosciences) using CellQuest software and analyzed with FlowJo software, using Abs obtained from BD Pharmingen.

Results

CCL21 and CCL19 induce chemokinesis in resting $CD4^+$ T cells exposed to an adhesive substrate

Many chemokines, including CCL19 and CCL21, are known to trigger polarization in resting T cells at uniform concentrations (16, 17). We confirmed that both CCL21 (Fig. 1, *A* and *B*) and CCL19 (data not shown) elicited pronounced polarization of ~75% of freshly isolated murine (C57BL/6 strain) $CD4^+$ T cells within 5 min, whereas the majority of untreated resting cells were round. In experiments where $CD62L^+CD44^{low}$, $CD62L^+CD44^{high}$, and $CD62L^-CD4$ T cells were separated, all populations responded nearly equally to CCL21 (data not shown). When T cells were seeded on bare glass with soluble CCL21 and

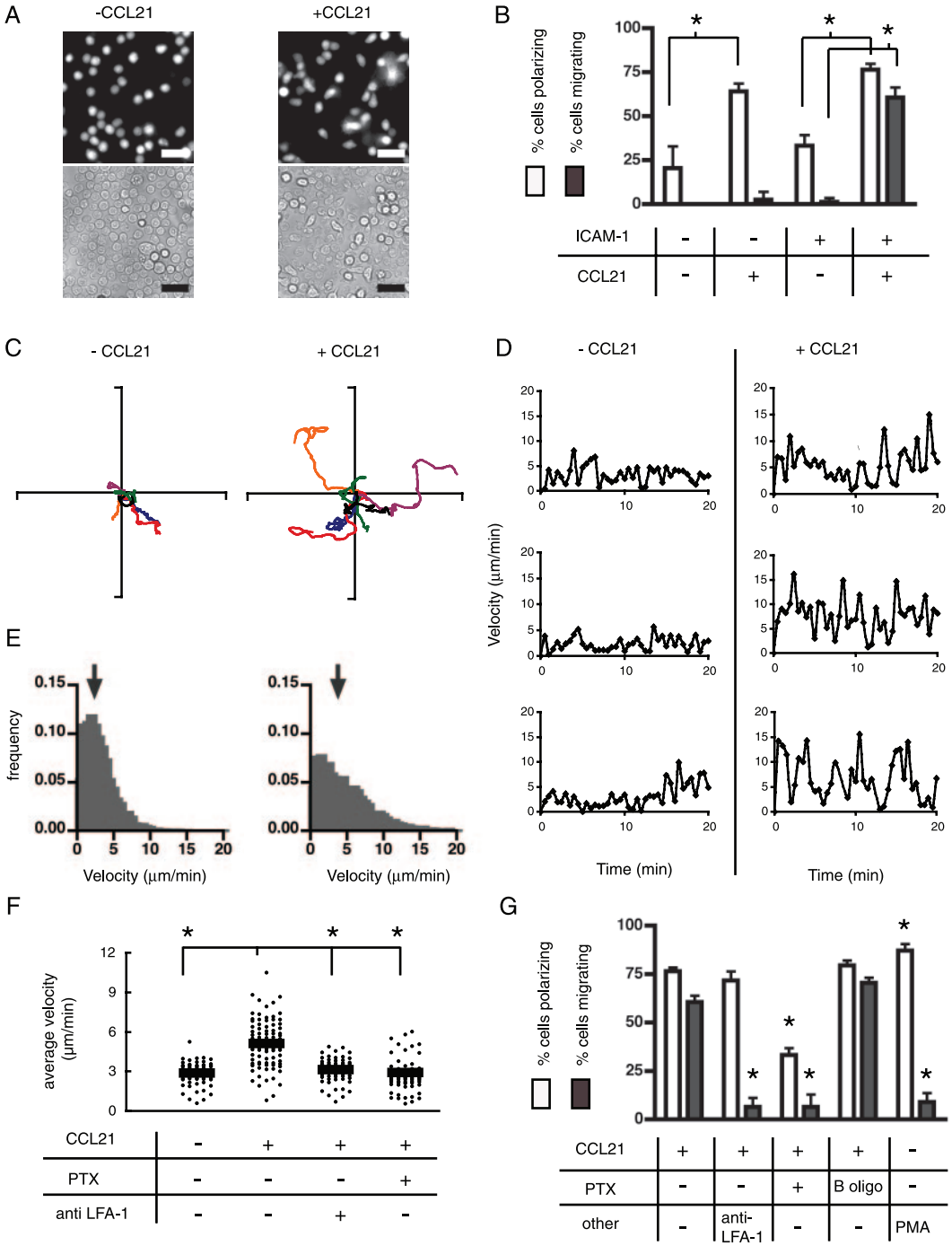

FIGURE 1. CCL21 synergizes with ICAM-1 to promote chemokinesis of freshly isolated CD4$^+$ T cells. *A*, Fluorescence (top) and brightfield (bottom) images of C57BL/6 CD4$^+$ T cells before (left) and 20 min after (right) addition of 1 μg/ml CCL21. A fraction of cells (20%) were labeled with fura 2-AM for software-assisted tracking. Scale bars, 20 μm. *B*, Percentage of T cells polarizing and migrating on bare or ICAM-1-coated surfaces, with or without CCL21 addition. The average $\pm$ SD is shown for three independent experiments per condition. $*$, Bracketed conditions are statistically different ($p \leq 0.05$). *C*, Two-dimensional migration paths for six representative control (*left*) and CCL21-stimulated (*right*) cells over 20 min are shown; all axes, 90 μm. *D*, Single-cell velocity time courses for three of the individual control (*left*) and CCL21-stimulated (*right*) cell tracks shown in *C*. *E*, Instantaneous velocity distributions on ICAM-1-coated surfaces without (left) or with (right) CCL21 are shown ($n > 75$ cells each). *F*, Time-averaged single-cell velocities on ICAM-1 surfaces with or without CCL21 addition and other treatments as shown; bars indicate the population average velocity. $*$, conditions statistically different ($p \leq 0.0001$) from +CCL21 sample. *G*, Percentage of T cells polarizing and migrating on ICAM-1-coated surfaces after indicated treatments shown for three independent experiments per condition. $*$, statistically different ($p \leq 0.05$) from +CCL21 only case.

tracked by videomicroscopy, we observed not only rapid cell polarization, but also that a small fraction of cells (~3%) appeared to actively migrate (Fig. 1*B*). Because polarization and adhesion are two prerequisites for T cell motility (6, 18), and CCL21 is known to induce adhesion to integrin ligands (19, 20), we tested whether motility would follow polarization if the cells were exposed to a suitable adhesive substrate.

CD4$^+$ T cells were seeded at relatively high densities (crudely mimicking the dense cellularity of SLO) on glass substrates coated with recombinant ICAM-1, with or without chemokine. T cells had

low basal adhesion and motility when seeded on ICAM-1-coated substrates in the absence of chemokine; most cells moved only by convective drift and collisions with neighboring cells (Fig. 1*B*, data not shown). In contrast, addition of CCL21 stimulated migration in 60 ± 5% of T cells (Fig. 1*B*). As illustrated by single-cell migration paths (Fig. 1*C*), CCL21-treated cells migrated substantial distances on ICAM-1 with no preferred direction, whereas the majority of cells remained relatively stationary in the absence of chemokine or slowly convected. Convecting vs migrating cells were readily distinguished via single-cell velocity time courses (Fig. 1*D*) and histograms of instantaneous velocities (Fig. 1*E*); migrating T cells had peak speeds of up to 20 μm/min, whereas control cells had smoother velocity profiles with speeds rarely exceeding 10 μm/min. The time-averaged velocity of single cells exposed to CCL21 on ICAM-1-coated surfaces ($\langle v \rangle$ = 5.16 ± 2.08 μm/min) was likewise significantly higher ($p \leq 0.0001$) than that observed for cells on ICAM-1 with no chemokine (Fig. 1*F*).

Importantly, chemokinetic migration was dependent on the presence of both chemokine and adhesive ligand: when the T cell integrin LFA-1 was blocked with an Ab, T cells on ICAM-1 substrates polarized, but failed to migrate (Fig. 1*G*); isotype control Ab had no effect (data not shown). Treatment of T cells with PTX, which inhibits G-protein-coupled receptor signaling, reduced both polarization and migration ($p \leq 0.05$), whereas the PTX B oligomer (control) had no effect (Fig. 1*G*). Blocking LFA-1-ICAM-1 interactions with an anti-LFA-1 Ab or treating the cells with PTX significantly reduced average cell velocities as well (Fig. 1*F*). We tested whether the observed migration was a result primarily of increased adhesion to ICAM-1 rather than chemokinesis per se, by treating cells with the phorbol ester PMA, which increases T cell adhesion to ICAM-1 (21). PMA triggered polarization in a majority of cells, but did not induce migration on ICAM-1 (Fig. 1*G*). Thus, CCL21 elicits chemokinesis from $CD4^+$ T cells, with migration dependent upon G-protein-coupled receptor signaling and exposure to an adhesive substrate such as ICAM-1.

Chemokinesis occurs at physiological CCL21 doses and supports long-lived cell migration

Naive T cells are estimated to spend 12–18 h in a single lymph node during their homeostatic recirculation between blood and secondary lymphoid tissues (9). For chemokinesis triggered by CCL21 to be relevant to T cells' search for Ag in lymph nodes, the migratory response would need to be sustained throughout a similar time period in response to chemokine doses present in the intact tissues. The concentration of CCL21 in SLO has been estimated at ~2 and ~10 μg/ml by ELISA and Western blotting of tissue supernatants, respectively (22–24). Using videomicroscopy, we found an onset of T cell motility induced by 10–100 ng/ml CCL21, whereas the percentage of cells polarizing and migrating began to plateau between 100 and 1000 ng/ml (Fig. 2*A*). However, the average time that any particular cell spent polarized and the average single-cell velocity continued to increase up to at least 10 μg/ml (data not shown). Notably, the onset and plateau response in chemokinetic migration measured here parallels the dose response reported for chemotactic migration triggered by murine CCL21 (25).

To assess the longevity of the observed chemokinetic response, T cells seeded on ICAM-1 surfaces were tracked by videomicroscopy 20 min after addition of CCL21, and again 24 h later. Live T cell migration in response to CCL21 did not appear to weaken at all over 1 day (Fig. 2, *B–D*), whereas only minor basal motility (<20%) developed in samples not treated with CCL21 (Fig. 2*B*). When we attempted to wash out the chemokine 24 h after addition

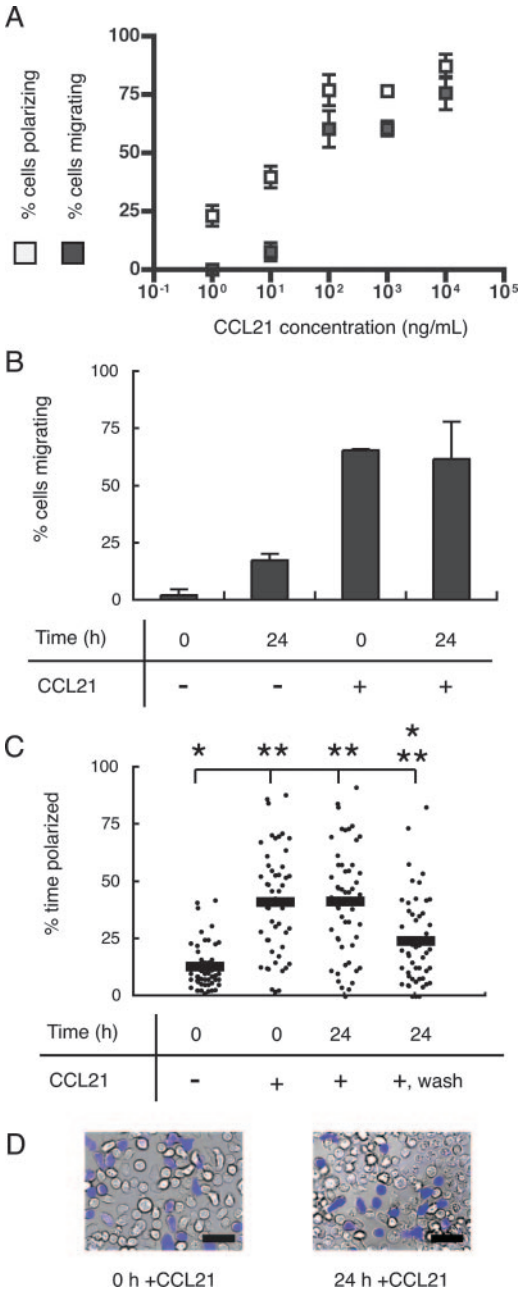

FIGURE 2. Polarization and migration responses of $CD4^+$ T cells triggered by CCL21 are sustained for at least 24 h in the presence of chemokine. A, Average percentage of cells polarizing and migrating at given doses of CCL21. *B*, Average percentage of cells migrating at 0 and 24 h in the presence or absence of chemokine (error bars represent range). *C*, Percentage of time polarized for individual cells from two pooled longevity and chemokine removal experiments: cells were observed at 0 h both before and after chemokine addition, 24 h later, and finally after washing. Horizontal bars denote population averages. * and **, conditions statistically different from +CCL21 ($p \leq 0.0001$) or control ($p \leq 0.001$) samples, respectively. *D*, For a sample treated with 1 μg/ml CCL21 at 0 h (left), many polarized cells remain at 24 h (right). Labeled cells (fura 2-AM) shown in false color. Scale bars, 20 μm.

(or 1 h; not shown), cell polarization was significantly reduced ($p \leq 0.0001$; Fig. 2*C*). Thus, CCL21-driven responses are sustained at physiological concentrations over time periods consistent with lymphocyte residence in a given lymph node and appear to be dependent on the persistent presence of chemokine.

CCL21 triggers chemokinesis on several adhesion ligands present in secondary lymphoid tissues

To determine whether CCL21 could synergize with other adhesion ligands present within T cell areas of SLO to promote T cell migration, we observed $CD4^+$ T cell motility on VCAM-1 and FN-coated substrates for comparison to the response observed on ICAM-1 surfaces. T cell polarization induced by CCL21 was statistically identical on bare glass or in the presence of each adhesion ligand (Fig. 3*A*). For all four surfaces, the population time-averaged velocity was increased in the presence of CCL21 (Fig. 3*B*). (This was true even on bare glass where cells were non-adherent, due to increased convection caused by CCL21-induced polarization.) However, the CCL21-induced increase in mean velocity of T cells was significantly greater for cells cultured on ICAM-1, VCAM-1, and FN compared with bare glass, suggesting that CCL21 can synergize with multiple adhesion ligands to promote T cell migration (Fig. 3*B*; $p \leq 0.05$). The exact velocity profiles of both chemokine-treated and untreated cells depended on the surface (Fig. 3*C*); this is to be expected, because cell migration rates are controlled by adhesion strength—which likely differs for each ligand at the single surface-coating densities tested here—as well as potential qualitative differences in the adhesion receptors involved (26). However, the responses measured here clearly indicate that chemokinesis induced by CCL21 in concert with an adhesive substrate is not limited to synergy with ICAM-1 alone.

CCL21 impacts $CD4^+$ T cell priming under conditions of rare Ag-specific T cell-DC encounters

To determine whether CCL21 could impact naive T cell priming under conditions modeling the rarity of Ag-specific encounters in vivo, we prepared T cell-DC cocultures where both Ag-specific T cells and peptide-bearing DCs were present at high dilution. We first assayed T cell activation kinetics via CD69 up-regulation, reasoning that chemokinesis triggered by CCL21 might alter the rate of early priming events. Peptide-loaded mature bone marrow-derived DCs (OVA-mDC) were mixed with peptide-free iDC at a ratio of 1:20 and plated in FN-coated round-bottom culture wells. A mixture of OVA peptide-specific transgenic $CD4^+$ T cells (OT-II) (27) and $CD4^+$ T cells from wild-type (C57BL/6) mice (at a 1:9 ratio) was then added for an overall 1:1 T/DC ratio. Wells received CCL21 (1 μg/ml) at both 0 and 48 h or were left untreated, and CD69 up-regulation was assessed as a function of time on equal numbers of live Ag-specific cells (identified as $CD4^+V\alpha2^+PI^{low}$ cells, a gating that included some wild-type cells) (Fig. 4*A*). As shown in Fig. 4*B* for a representative experiment, the fraction of $CD69^{high}$ $V\alpha2^+$ cells was higher for CCL21-treated samples than for untreated controls at all time points, by up to 1.5-fold at 48 h.

To distinguish between effects of CCL21 on T cells and DCs in the coculture, we also applied a PTX treatment strategy reported by Lo et al. (28) to block G-protein-coupled receptor signaling in a selected cell population for at least 26 h. PTX-treated T cells showed reduced CD69 up-regulation compared with untreated T cells in the presence of CCL21, indicating that the primary effect of CCL21 in these cocultures was mediated by T cells (Fig. 4*B*). The increase in the $CD69^{high}$ population elicited by CCL21 was significantly greater for untreated vs PTX-treated cocultures across multiple experiments ($p \leq 0.05$; Fig. 4*C*) and was most prominent at 48 h.

To examine the end-point effects of CCL21 on T cell priming, we performed a CFSE dilution assay to directly observe Ag-specific cell division. For this assay, OT-II T cells were again diluted 1:9 with polyclonal $CD4^+$ T cells, but a more physiological total

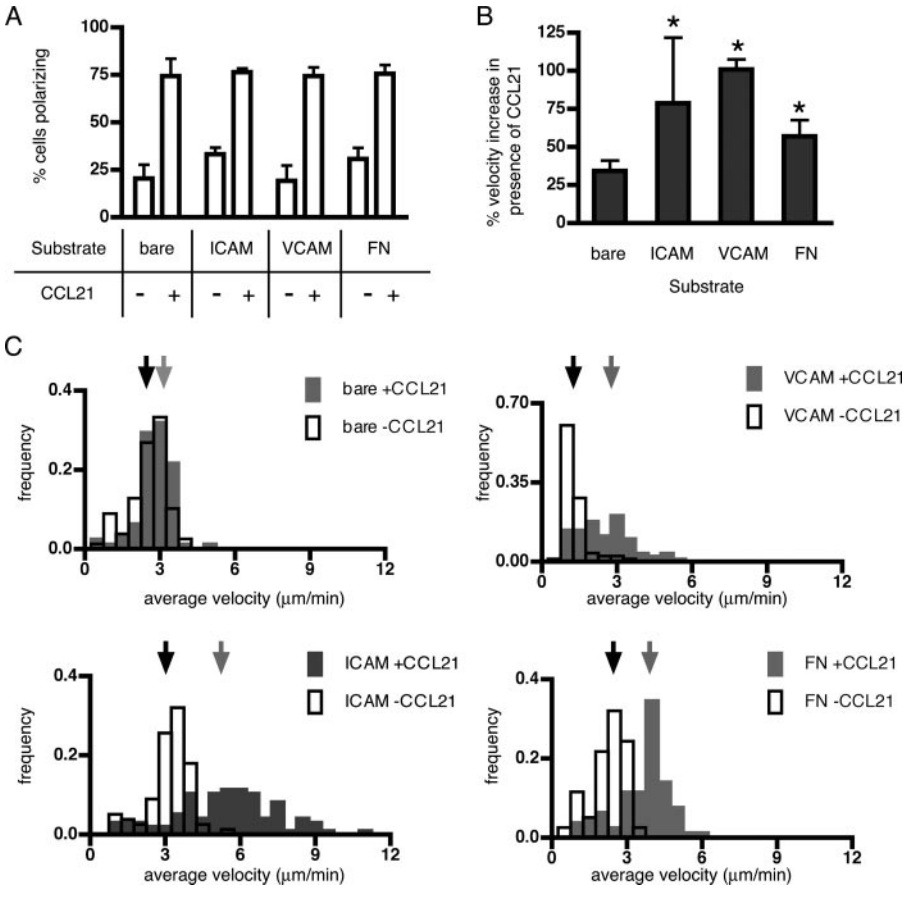

FIGURE 3. CCL21 synergizes with several adhesion ligands present in secondary lymphoid tissues to promote random T cell motility. A, Percentage of $CD4^+$ T cells polarizing on bare glass, ICAM-1-, VCAM-1-, or FN-coated substrates with/without CCL21. *B*, For each substrate, percentage of increase in average cell velocity with chemokine treatment (vs untreated sample) is shown. *, statistically different ($p \leq 0.05$) from bare glass case. *A* and *B*, Average ± SD for three independent experiments. *C*, Histograms of time-averaged single cell velocities for control and CCL21-stimulated cells on ICAM-1, VCAM-1, FN, and bare glass shown for three pooled experiments per condition ($n > 75$ cells each); arrows indicate population median velocity. CCL21 was used at 1 μg/ml for all experiments.

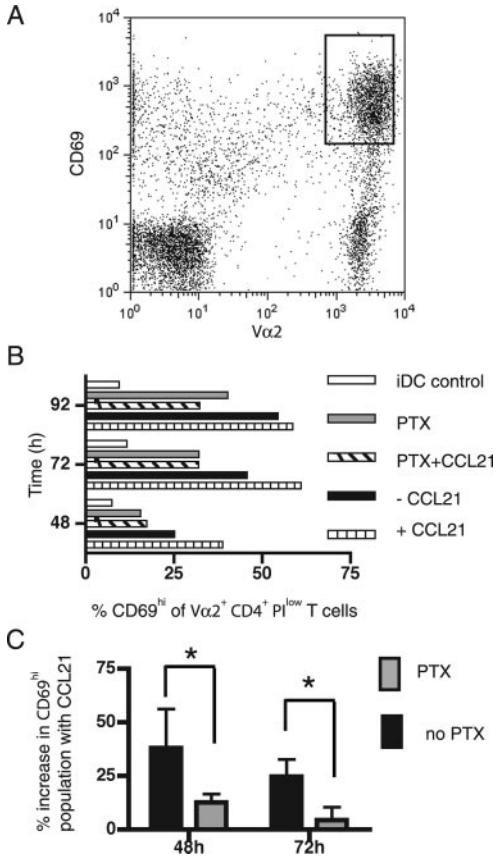

FIGURE 4. CCL21 impacts kinetics of naive T cell priming under conditions of rare Ag-specific T cell-rare Ag-bearing DC encounters. *A*—*C*, Cocultures comprising 5% OVA-specific OT-II $CD4^+$ T cells, 45% C57BL/6 $CD4^+$ T cells, 2.5% OVA-pulsed mature bone marrow-derived DC (OVA-mDC), and 47.5% iDC with/without CCL21 were analyzed by flow cytometry at the indicated times. *A*, $V\alpha2^+CD69^{high}$ cells from the $CD4^+PI^{low}$ population were identified as shown by the rectangular gate. *B*, Percentage of $CD69^{high}$ of $V\alpha2^+$ T cells over time for control (−CCL21), CCL21-treated (+CCL21), PTX-treated cells and without CCL21, and a control containing 50% T cells and 50% iDC are shown. *A* and *B* are data from one representative of three independent experiments. *C*, Percentage of increase in $CD69^{high}$ population for CCL21-treated samples (vs relevant control), comparing PTX-treated (gray) and untreated (black) samples; data from three independent experiments, pooled. ∗, bracketed samples statistically different ($p \leq 0.05$).

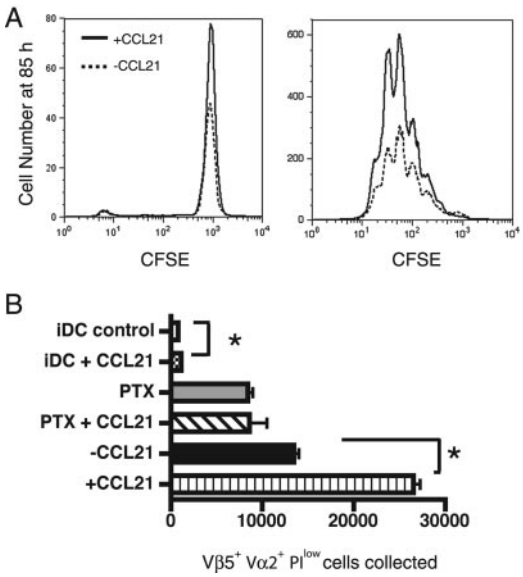

FIGURE 5. CCL21 impacts naive T cell proliferation under conditions of rare Ag-specific T-DC encounters. Cocultures comprising 9% OVA-specific OT-II $CD4^+$ T cells, 81% C57BL/6 $CD4^+$ T cells, 5% OVA-mDC, and 5% iDC with/without CCL21 were analyzed by flow cytometry at 85 h. *A*, Sample CFSE histograms are shown for control (left, iDC only) and experimental (right, with OVA-mDC) conditions. *B*, OT-II cell recovery for all conditions is shown. Average ± SD for 3 wells per condition. ∗, bracketed conditions statistically different ($p \leq 0.05$). *A* and *B*, from one representative of five experiments.

T/DC ratio of 9:1 was used, and the DC population was equal parts iDC and OVA-mDC. OT-II T cells in the culture were labeled with CFSE to track cell division by flow cytometry. At 85 h, equal volumes of total cells were analyzed, and the number of live OT-II cells ($V\alpha2^+V\beta5^+PI^{low}$) and their CFSE fluorescence distribution were determined. In control cocultures where all DCs were immature cells lacking Ag, no cell division was observed; in contrast, both PTX-treated and untreated OT-II cells proliferated when OVA-mDC were present (Fig. 5*A* and data not shown), with similar cell division profiles irrespective of CCL21 treatment (2.88 ± 0.03 vs 2.70 ± 0.02 mean divisions per cell in the presence or absence of chemokine, respectively, for the OVA-mDC case). Equal numbers of OT-II cells were recovered from PTX-treated samples regardless of CCL21 treatment (Fig. 5*B*). However, in both the presence and absence of OVA-mDC, the addition of CCL21 increased the number of OT-II T cells recovered significantly, by 2.0- and 1.4-fold, respectively ($p \leq 0.05$; Fig. 5*B*). In comparing multiple similar experiments, we found that the fold increase in T cell recovery was consistently greater in the presence of Ag-bearing DCs than in their absence (2.1 ± 0.4-fold in the presence of Ag, 1.4 ± 0.1-fold in the absence of Ag, $p \leq 0.05$), thus showing an Ag-specific effect. The enhanced cell recovery in CCL21-treated cocultures was not due to a direct survival signal delivered to resting T cells by chemokine, as purified T cells cultured alone for 24 h with or without CCL21 were recovered in equal numbers (data not shown). Altogether, these results suggest that CCL21 signaling can impact the kinetics of early activation events and the ultimate number of expanded T cells while having a minor impact on the mean number of cell divisions, under conditions where Ag-specific T cells and peptide-bearing DCs are present at low frequency.

B cells exhibit chemokinesis in response to CXCL13

The data presented above show strong chemokinesis induced in $CD4^+$ T cells by CCL21, a chemokine produced constitutively at high levels in the T cell areas of SLO (9). To determine whether chemokinesis is also a potential regulatory mechanism in B cell areas of SLO, we tested whether CXCL13, produced constitutively in follicles, would elicit an analogous response in B lymphocytes. B cells isolated from C57BL/6 mice were seeded on ICAM-1-coated substrates with or without CXCL13 and tracked by video-microscopy as above. Like $CD4^+$ T cells, B cells displayed low motility on ICAM-1 surfaces, but cell polarization and migration increased dramatically on exposure to CXCL13 ($\langle v \rangle = 4.10 \pm 1.58$ μm/min) (Fig. 6*A*). PTX treatment blocked this response to CXCL13 completely, whereas treatment of cells with PTX B oligomer had almost no effect. Analogous to T cells, treatment with the nonspecific adhesion stimulus PMA caused polarization but did not induce migration. However, in contrast to T cell responses to CCL21, anti-LFA-1 treatment suppressed both CXCL13-induced migration and polarization. To rule out potential nonspecific effects of coating the cells with the blocking Ab or FcR signaling in the cells, we also compared the response of cells treated with an

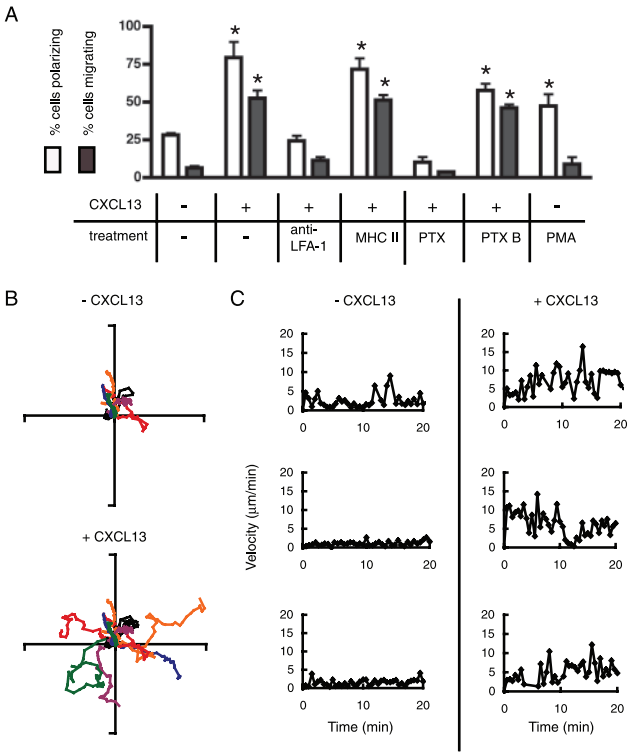

FIGURE 6. CXCL13 triggers chemokinesis in B cells. A, Percentage of B cells polarizing and migrating on ICAM-1-coated surfaces, with or without CXCL13 and other treatments as shown. Average ± SD shown for three experiments per condition. ∗, statistically different ($p \leq 0.05$) from control sample. *B*, B cell migration paths for 6 cells over 20 min in control (top) and CXCL13-stimulated (bottom) conditions; axes, 50 μm. C, Velocity time course of three representative cells seeded on ICAM-1 surfaces in the presence or absence of CXCL13. CXCL13 used at 1 μg/ml in all experiments.

isotype-matched anti-I-A^b (Fig. 6*A*); in this case B cell polarization and migration was not statistically different from untreated cells. (A non-binding isotype control Ab also failed to block CXCL13 responses; data not shown). These results suggest that in B cells, both polarization and migration on ICAM-1 are governed by a synergy between chemokine and LFA-1 signaling. Little movement of B cells from their point of origin was observed on ICAM-1 in the absence of chemokine, but single cell tracks revealed significant random motility upon addition of CXCL13, with peak instantaneous velocities >15 μm/min and average velocities of 4.10 ± 1.58 μm/min (Fig. 6, *B* and *C*). Thus, B cells respond to synergistic signaling from CXCL13 and ICAM-1 and exhibit chemokinetic migration in a manner largely analogous to the response of T cells to CCL21 and ICAM-1.

Discussion

Fewer than 1 in 1000 naive T cells express receptors specific for any given Ag (29, 30), and for a primary immune response to occur, these scarce Ag-specific T cells must come into physical contact with rare but strategically placed DCs (31, 32). Furthermore, during Ag-limited infections or immunizations, only a fraction of DCs may present the relevant Ag to T cells. Recent studies have revealed sphingosine-1 phosphate receptor down-modulation on entry into lymph nodes and slow re-expression during trafficking through the lymphoid tissue as a possible molecular timer influencing naive T cell residence times in lymph nodes (28). Rapid motility within lymph nodes may thus enable efficient detection of rare Ags before default trafficking of Ag-specific cells out of the organ. Here we tested whether chemokinesis could be one regulatory mechanism in SLO for inducing favorable motility during both T cell priming and homeostatic trafficking.

We first showed, using direct videomicroscopic observation, that the homeostatic chemokine most abundant in T cell areas of SLO—CCL21—causes pronounced T cell migration in the absence of specific gradients and that this response is critically dependent on the presence of appropriate ligands to promote cell adhesion, notably ICAM-1. In secondary lymphoid tissues where CCL21 (and CCL19) is constitutively produced, T cells are exposed to VCAM-1 on stromal cells and DCs (33), ICAM-1 on DCs (34) and potentially stromal cells (33), and possibly FN presented by fibroblastic reticular cells or exposed on the surface of a small fraction of reticular fibers not enveloped by reticular cells (35, 36). We found that all three of these ligands could support some degree of cell migration. Highly favorable T cell migration on ICAM-1 may reflect the need for rapid investigation of DC cell bodies. Notably, histological studies reveal that ~60% of T cells in lymph nodes are in contact with DCs at any given moment (31).

For chemokinesis to be relevant for T cell migration within SLO, it should be sustained for the typical cell residence time: 12–18 h in the case of lymph nodes (9). We found that CCL21-induced chemokinesis is indeed sustained for at least 24 h, consistent with the finding in the human system that, in contrast to many chemokine/receptor interactions, CCL21 binding to CCR7 does not trigger receptor down-modulation (37). The residual cell polarization we observed after washing out chemokine may be due to the high-affinity nature of CCL21-CCR7 binding and possible chemokine sequestration by cell surface proteoglycans (38, 39), which complicate full separation of the cells from ligand. Nevertheless, we observed that the long-term chemokinetic response was dependent at least in part on the continued presence of CCL21.

Based on these findings, we sought to examine whether chemokinesis triggered by CCL21 could impact T cell priming, using a culture system designed to model the infrequency of Ag-specific T-DC contacts in vivo. We found that addition of CCL21 to T cell-DC cocultures enhanced the initial kinetics of CD69 up-regulation and led to 2-fold greater numbers of Ag-specific OT-II T cells recovered after 4 days. Because activated/expanded T cells are constitutively motile (40–43), we might expect that the presence of CCL21 would only alter the initial number of (otherwise non-motile) naive T cells that would encounter a DC and begin proliferating. Naive cells that did make contact with DCs and divide (in the presence or absence of chemokine) would thus proceed at equal rates to begin dividing, assuming equal rates of further cell division and no differences in cell death (we found similar fractions of apoptotic cells in cultures with or without CCL21, data not shown). In agreement with this hypothesis, CCL21-treated T cells had similar cell division profiles as control cells—only the recovery of Ag-specific T cells changed. Surprisingly, we found that addition of CCL21 to peptide-free cocultures also increased the recovery of OT-II cells, though control experiments revealed no evidence for a direct survival signal given to T cells by CCL21 (data not shown). This could be due to CCL21-driven T cell motility increasing Ag-independent T-DC contacts, which promote T cell survival (44, 45). We found that the increase in T cell recovery was consistently greater in the presence of Ag-bearing DCs than in their absence, suggesting an Ag-specific effect apart from survival cues imparted to T cells by immature DCs.

These results suggested an influence of T cell chemokinesis on priming but were not definitive, since the receptor for CCL21, CCR7, is expressed by both naive T cells and mature DCs (46),

and CCR7 signaling is known to promote DC motility (47), dendrite extension (48), and enhance LPS-driven maturation (49). However, flow cytometry analysis of our LPS-matured DCs exposed to the prokaryotic-derived CCL21 used here showed no evidence of further maturation, nor were immature DCs matured by CCL21 (data not shown). More importantly, selective PTX treatment of T cells alone largely abrogated the positive effects of CCL21 (Figs. 4, *B* and *C*, and 5*B*), suggesting that chemokine receptor signaling in T cells was responsible for the accelerated CD69 up-regulation and enhanced proliferation of Ag-specific cells in our coculture system. Notably, CD69 up-regulation and proliferation of PTX-treated cells were slightly lower than for untreated T cells even in the absence of exogenously added CCL21 (Figs. 4, *B* and *C*, and 5*B*), perhaps reflecting a contribution of other chemokine signals to the T cell response—e.g., CCL19, which is produced by mature DCs (50) and which has recently been shown by Kaiser et al. to promote T cell scanning of DCs (8).

Finally, we examined whether B lymphocytes exposed to the follicular homeostatic chemokine CXCL13 would have a chemokinetic response analogous to T cells. B cells on ICAM-1 surfaces were indeed stimulated to migrate by CXCL13. Consistent with the slower velocities of B cells relative to T cells reported by imaging of intact lymphoid tissues (2, 51), the population average velocity and peak velocities of single cells were lower for B cells treated with CXCL13 than for $CD4^+$ T cells responding to CCL21.

Altogether, these findings suggest that the rapid migration of lymphocytes observed within the parenchyma of SLO could be supported by chemokine signaling in the absence of significant concentration gradients. Recent analyses of T cell migration within intact SLO have so far failed to reveal evidence for chemotaxis during homeostatic lymphocyte trafficking once T and B cells reach their respective zones, which may reflect a truly random program for T cell scanning or the action of very local attraction gradients near APCs (1, 2, 4). In either case, the data shown here suggest that homeostatic chemokines could function not only to direct lymphocytes to their respective compartments but also to regulate the random motility of these cells in lymphoid organs observed during their constitutive surveillance for Ag.

Acknowledgments

We thank Nir Hacohen for helpful discussions and Glenn Paradis at the MIT Flow Cytometry Core Facility for technical assistance.

Disclosures

The authors have no financial conflict of interest.

References

1. Miller, M. J., S. H. Wei, M. D. Cahalan, and I. Parker. 2003. Autonomous T cell trafficking examined in vivo with intravital two-photon microscopy. *Proc. Natl. Acad. Sci. USA* 100: 2604–2609.
2. Okada, T., M. J. Miller, I. Parker, M. F. Krummel, M. Neighbors, S. B. Hartley, A. O'Garra, M. D. Cahalan, and J. G. Cyster. 2005. Antigen-engaged B cells undergo chemotaxis toward the T zone and form motile conjugates with helper T cells. *PLoS Biol.* 3: e150.
3. Bousso, P., and E. Robey. 2003. Dynamics of CD8+ T cell priming by dendritic cells in intact lymph nodes. *Nat. Immunol.* 4: 579–585.
4. Sumen, C., T. R. Mempel, I. B. Mazo, and U. H. von Andrian. 2004. Intravital microscopy: visualizing immunity in context. *Immunity* 21: 315–329.
5. Huang, A. Y., H. Qi, and R. N. Germain. 2004. Illuminating the landscape of in vivo immunity: insights from dynamic in situ imaging of secondary lymphoid tissues. *Immunity* 21: 331–339.
6. Negulescu, P. A., T. B. Krasieva, A. Khan, H. H. Kerschbaum, and M. D. Cahalan. 1996. Polarity of T cell shape, motility, and sensitivity to antigen. *Immunity* 4: 421–430.
7. Wilkinson, P. C. 1986. The locomotor capacity of human lymphocytes and its enhancement by cell growth. *Immunology* 57: 281–289.
8. Kaiser, A., E. Donnadieu, J. P. Abastado, A. Trautmann, and A. Nardin. 2005. CC chemokine ligand 19 secreted by mature dendritic cells increases naive T cell scanning behavior and their response to rare cognate antigen. *J. Immunol.* 175: 2349–2356.
9. Cyster, J. G. 2005. Chemokines, sphingosine-1-phosphate, and cell migration in secondary lymphoid organs. *Annu. Rev. Immunol.* 23: 127–159.
10. Yoshida, R., M. Nagira, T. Imai, M. Baba, S. Takagi, Y. Tabira, J. Akagi, H. Nomiyama, and O. Yoshie. 1998. EBI1-ligand chemokine (ELC) attracts a broad spectrum of lymphocytes: activated T cells strongly up-regulate CCR7 and efficiently migrate toward ELC. *Int. Immunol.* 10: 901–910.
11. Gunn, M. D., V. N. Ngo, K. M. Ansel, E. H. Ekland, J. G. Cyster, and L. T. Williams. 1998. A B-cell-homing chemokine made in lymphoid follicles activates Burkitt's lymphoma receptor-1. *Nature* 391: 799–803.
12. Campbell, J. J., E. P. Bowman, K. Murphy, K. R. Youngman, M. A. Siani, D. A. Thompson, L. Wu, A. Zlotnik, and E. C. Butcher. 1998. 6-C-kine (SLC), a lymphocyte adhesion-triggering chemokine expressed by high endothelium, is an agonist for the MIP-3beta receptor CCR7. *J. Cell Biol.* 141: 1053–1059.
13. Frow, E. K., J. Reckless, and D. J. Grainger. 2004. Tools for anti-inflammatory drug design: in vitro models of leukocyte migration. *Med. Res. Rev.* 24: 276–298.
14. Dunzendorfer, S., A. Kaser, C. Meierhofer, H. Tilg, and C. J. Wiedermann. 2000. Dendritic cell migration in different micropore filter assays. *Immunol. Lett.* 71: 5–11.
15. Inaba, K., M. Inaba, N. Romani, H. Aya, M. Deguchi, S. Ikehara, S. Muramatsu, and R. M. Steinman. 1992. Generation of large numbers of dendritic cells from mouse bone marrow cultures supplemented with granulocyte/macrophage colony-stimulating factor. *J. Exp. Med.* 176: 1693–1702.
16. Nombela-Arrieta, C., R. A. Lacalle, M. C. Montoya, Y. Kunisaki, D. Megias, M. Marques, A. C. Carrera, S. Manes, Y. Fukui, A. C. Martinez, and J. V. Stein. 2004. Differential requirements for DOCK2 and phosphoinositide-3-kinase gamma during T and B lymphocyte homing. *Immunity* 21: 429–441.
17. Brown, M. J., R. Nijhara, J. A. Hallam, M. Gignac, K. M. Yamada, S. L. Erlandsen, J. Delon, M. Kruhlak, and S. Shaw. 2003. Chemokine stimulation of human peripheral blood T lymphocytes induces rapid dephosphorylation of ERM proteins, which facilitates loss of microvilli and polarization. *Blood* 102: 3890–3899.
18. Dustin, M. L., and J. A. Cooper. 2000. The immunological synapse and the actin cytoskeleton: molecular hardware for T cell signaling. *Nat. Immunol.* 1: 23–29.
19. Bromley, S. K., and M. L. Dustin. 2002. Stimulation of naive T-cell adhesion and immunological synapse formation by chemokine-dependent and -independent mechanisms. *Immunology* 106: 289–298.
20. Laudanna, C., J. Y. Kim, G. Constantin, and E. Butcher. 2002. Rapid leukocyte integrin activation by chemokines. *Immunol. Rev.* 186: 37–46.
21. Dustin, M. L., and T. A. Springer. 1989. T-cell receptor cross-linking transiently stimulates adhesiveness through LFA-1. *Nature* 341: 619–624.
22. Stein, J. V., A. Rot, Y. Luo, M. Narasimhaswamy, H. Nakano, M. D. Gunn, A. Matsuzawa, E. J. Quackenbush, M. E. Dorf, and U. H. von Andrian. 2000. The CC chemokine thymus-derived chemotactic agent 4 (TCA-4, secondary lymphoid tissue chemokine, 6Ckine, exodus-2) triggers lymphocyte function-associated antigen 1-mediated arrest of rolling T lymphocytes in peripheral lymph node high endothelial venules. *J. Exp. Med.* 191: 61–76.
23. Fan, L., C. R. Reilly, Y. Luo, M. E. Dorf, and D. Lo. 2000. Cutting edge: ectopic expression of the chemokine TCA4/SLC is sufficient to trigger lymphoid neogenesis. *J. Immunol.* 164: 3955–3959.
24. Luther, S. A., A. Bidgol, D. C. Hargreaves, A. Schmidt, Y. Xu, J. Paniyadi, M. Matloubian, and J. G. Cyster. 2002. Differing activities of homeostatic chemokines CCL19, CCL21, and CXCL12 in lymphocyte and dendritic cell recruitment and lymphoid neogenesis. *J. Immunol.* 169: 424–433.
25. Gunn, M. D., K. Tangemann, C. Tam, J. G. Cyster, S. D. Rosen, and L. T. Williams. 1998. A chemokine expressed in lymphoid high endothelial venules promotes the adhesion and chemotaxis of naive T lymphocytes. *Proc. Natl. Acad. Sci. USA* 95: 258–263.
26. Palecek, S. P., J. C. Loftus, M. H. Ginsberg, D. A. Lauffenburger, and A. F. Horwitz. 1997. Integrin-ligand binding properties govern cell migration speed through cell-substratum adhesiveness. *Nature* 385: 537–540.
27. Barnden, M. J., J. Allison, W. R. Heath, and F. R. Carbone. 1998. Defective TCR expression in transgenic mice constructed using cDNA-based alpha- and beta-chain genes under the control of heterologous regulatory elements. *Immunol. Cell Biol.* 76: 34–40.
28. Lo, C. G., Y. Xu, R. L. Proia, and J. G. Cyster. 2005. Cyclical modulation of sphingosine-1-phosphate receptor 1 surface expression during lymphocyte recirculation and relationship to lymphoid organ transit. *J. Exp. Med.* 201: 291–301.
29. von Andrian, U. H., and C. R. Mackay. 2000. T-cell function and migration. Two sides of the same coin. *N. Engl. J. Med.* 343: 1020–1034.
30. Blattman, J. N., R. Antia, D. J. Sourdive, X. Wang, S. M. Kaech, K. Murali-Krishna, J. D. Altman, and R. Ahmed. 2002. Estimating the precursor frequency of naive antigen-specific CD8 T cells. *J. Exp. Med.* 195: 657–664.
31. Westermann, J., U. Bode, A. Sahle, U. Speck, N. Karin, E. B. Bell, K. Kalies, and A. Gebert. 2005. Naive, effector, and memory T lymphocytes efficiently scan dendritic cells in vivo: contact frequency in T cell zones of secondary lymphoid organs does not depend on LFA-1 expression and facilitates survival of effector T cells. *J. Immunol.* 174: 2517–2524.
32. Lindquist, R. L., G. Shakhar, D. Dudziak, H. Wardemann, T. Eisenreich, M. L. Dustin, and M. C. Nussenzweig. 2004. Visualizing dendritic cell networks in vivo. *Nat. Immunol.* 5: 1243–1250.
33. Katakai, T., T. Hara, M. Sugai, H. Gonda, and A. Shimizu. 2004. Lymph node fibroblastic reticular cells construct the stromal reticulum via contact with lymphocytes. *J. Exp. Med.* 200: 783–795.
34. de la Fuente, H., M. Mittelbrunn, L. Sanchez-Martin, M. Vicente-Manzanares, A. Lamana, R. Pardi, C. Cabanas, and F. Sanchez-Madrid. 2005. Synaptic clusters of MHC class II molecules induced on DCs by adhesion molecule-mediated initial T-cell scanning. *Molecular Biology of the Cell* 16: 3314–3322.

35. Gretz, J. E., A. O. Anderson, and S. Shaw. 1997. Cords, channels, corridors and conduits: critical architectural elements facilitating cell interactions in the lymph node cortex. *Immunol. Rev.* 156: 11–24.
36. Hayakawa, M., M. Kobayashi, and T. Hoshino. 1988. Direct contact between reticular fibers and migratory cells in the paracortex of mouse lymph nodes: a morphological and quantitative study. *Arch. Histol. Cytol.* 51: 233–240.
37. Bardi, G., M. Lipp, M. Baggiolini, and P. Loetscher. 2001. The T cell chemokine receptor CCR7 is internalized on stimulation with ELC, but not with SLC. *Eur. J. Immunol.* 31: 3291–3297.
38. Proudfoot, A. E., T. M. Handel, Z. Johnson, E. K. Lau, P. LiWang, I. Clark-Lewis, F. Borlat, T. N. Wells, and M. H. Kosco-Vilbois. 2003. Glycosaminoglycan binding and oligomerization are essential for the in vivo activity of certain chemokines. *Proc. Natl. Acad. Sci. USA* 100: 1885–1890.
39. Tanaka, Y., D. H. Adams, S. Hubscher, H. Hirano, U. Siebenlist, and S. Shaw. 1993. T-cell adhesion induced by proteoglycan-immobilized cytokine MIP-1 beta. *Nature* 361: 79–82.
40. Bromley, S. K., D. A. Peterson, M. D. Gunn, and M. L. Dustin. 2000. Cutting edge: hierarchy of chemokine receptor and TCR signals regulating T cell migration and proliferation. *J. Immunol.* 165: 15–19.
41. Ratner, S., R. K. Jasti, and G. H. Heppner. 1988. Motility of murine lymphocytes during transit through cell cycle. Analysis by a new in vitro assay. *J. Immunol.* 140: 583–588.
42. Smith, A., Y. R. Carrasco, P. Stanley, N. Kieffer, F. D. Batista, and N. Hogg. 2005. A talin-dependent LFA-1 focal zone is formed by rapidly migrating T lymphocytes. *J. Cell Biol.* 170: 141–151.
43. Volkov, Y., A. Long, S. McGrath, D. Ni Eidhin, and D. Kelleher. 2001. Crucial importance of PKC-beta(I) in LFA-1-mediated locomotion of activated T cells. *Nat. Immunol.* 2: 508–514.
44. Ge, Q., D. Palliser, H. N. Eisen, and J. Chen. 2002. Homeostatic T cell proliferation in a T cell-dendritic cell coculture system. *Proc. Natl. Acad. Sci. USA* 99: 2983–2988.
45. Kondo, T., I. Cortese, S. Markovic-Plese, K. P. Wandinger, C. Carter, M. Brown, S. Leitman, and R. Martin. 2001. Dendritic cells signal T cells in the absence of exogenous antigen. *Nat. Immunol.* 2: 932–938.
46. Dieu, M. C., B. Vanbervliet, A. Vicari, J. M. Bridon, E. Oldham, S. Ait-Yahia, F. Briere, A. Zlotnik, S. Lebecque, and C. Caux. 1998. Selective recruitment of immature and mature dendritic cells by distinct chemokines expressed in different anatomic sites. *J. Exp. Med.* 188: 373–386.
47. Riol-Blanco, L., N. Sanchez-Sanchez, A. Torres, A. Tejedor, S. Narumiya, A. L. Corbi, P. Sanchez-Mateos, and J. L. Rodriguez-Fernandez. 2005. The chemokine receptor CCR7 activates in dendritic cells two signaling modules that independently regulate chemotaxis and migratory speed. *J. Immunol.* 174: 4070–4080.
48. Yanagawa, Y., and K. Onoe. 2002. CCL19 induces rapid dendritic extension of murine dendritic cells. *Blood* 100: 1948–1956.
49. Marsland, B. J., P. Battig, M. Bauer, C. Ruedl, U. Lassing, R. R. Beerli, K. Dietmeier, L. Ivanova, T. Pfister, L. Vogt, H. Nakano, C. Nembrini, P. Saudan, M. Kopf, and M. F. Bachmann. 2005. CCL19 and CCL21 induce a potent proinflammatory differentiation program in licensed dendritic cells. *Immunity* 22: 493–505.
50. Katou, F., H. Ohtani, T. Nakayama, H. Nagura, O. Yoshie, and K. Motegi. 2003. Differential expression of CCL19 by DC-Lamp+ mature dendritic cells in human lymph node versus chronically inflamed skin. *J. Pathol.* 199: 98–106.
51. Miller, M. J., S. H. Wei, I. Parker, and M. D. Cahalan. 2002. Two-photon imaging of lymphocyte motility and antigen response in intact lymph node. *Science* 296: 1869–1873.